JJMIE

Volume 1, Number 2, Dec. 2007
ISSN 1995-6665
Pages 105 - 111

Jordan Journal of Mechanical and Industrial Engineering

Strain-Concentration Factor of Notched Cylindrical Austenitic Stainless Steel Bar with Double Slant Circumferential U-Notches Under Static Tension

Hitham M. Tlilan [a,*], Ahmad S. Al-Shyyab [a], Tariq Darabseh [b], Majima Tamotsu [c]

[a] Department of Mechanical Engg., Faculty of Engg., The Hashemite University, P.O. Box 330127, Zarqa 13133, Jordan
[b] Department of Mechanical Engg., Faculty of Engg., J.U.S.T, Irbid, 22110, Jordan
[c] Graduate School of Science and Technology, Chiba University, Chiba, 263-8522, Japan

Abstract

The interference effect on the new strain-concentration factor (SNCF), defined under the triaxial stress state, is studied for circumferentially notched cylindrical bars with double-slant notches under static tension. The material employed is Austenitic stainless steel. The results indicate that the new SNCF (K_ε^{new}) for a certain l_o is constant during elastic deformation and increases with decreasing pitch l_o. It also increases with increasing notch radius. The elastic K_ε^{new} for l_o = 0.5 mm is the minimum. This becomes prominent with decreasing notch radius. The new SNCF increases from its elastic value to a peak value as the plastic deformation develops from notch root. On further plastic deformation, the new SNCF increases to the maximum value for l_o = 0.0 and $l_o \geq 2.5$ and then decreases with plastic deformation. This peak value is the maximum K_ε^{new} for $0.0 < l_o \leq 2.0$.

Keywords: Austenitic stainless steel; interference; slanted notch; strain-concentration factor; tension;

Nomenclature

Alphabetic symbols

A	: net-section area
d_o	: initial net-section diameter
D_o	: initial gross diameter
E	: Young's modulus
K_ε^{con}	: conventional strain-concentration factor
K_ε^{new}	: new strain-concentration factor
P	: tensile load
P_Y	: tensile load at yielding at the notch root
r	: instantaneous distance from the center of the net-section ($0 \leq r \leq r_n$)
r_n	: instantaneous net-section radius = $d/2$
s	: = r/r_n ($0 \leq s \leq 1.0$)

Greek Symbols

ε_z	: axial strain
$(\varepsilon_z)_{av}^{con}$	: conventional average axial strain
$(\varepsilon_z)_{av}^{new}$	: new average axial strain
$(\varepsilon_z)_{max}$	: maximum axial strain
ν	: Poisson's ratio
ρ_o	: initial notch radius
σ_{eq}	: equivalent stress $= \left\{(\sigma_z-\sigma_\theta)^2+(\sigma_\theta-\sigma_r)^2+(\sigma_r-\sigma_z)^2\right\}^{1/2}/\sqrt{2}$
$(\sigma_{eq})_{max}$	: equivalent stress at the notch root
σ_r , σ_z , σ_θ	: radial , axial and tangential stresses
σ_Y	: yield stress
$(\sigma_z)_{av}$	: average axial stress at the net section = P/A
$(\sigma_z)_{max}$	: axial stress at the notch root in elastic deformation
$(\sigma_\theta)_{max}$	: tangential stress at the notch root in elastic deformation

1. Introduction

Geometrical irregularities, in the following referred to as notches, are of prime importance in the life assessment of machine elements, since they act as local stress and strain raisers. The presence of notches in machine element forms an interruption of the load path; it will, therefore, bring about stress and strain concentrations at the notch root. The knowledge of stress and strain distributions on the net section is valuable for practical design and application of various engineering elements. In addition to

* Corresponding author. e-mail: hitham@hu.edu.jo

the stress and strain concentrations introduced by the notch, there is also a change in the stress state even if the stress state is uniaxial throughout the remainder of the gage length. That is, the stress state becomes triaxial stress state in the immediate vicinity of the notch root.

Attempts have been made to predict the axial strain at the notch root under static and cyclic tensile loading. This prediction was made using the SNCF, referred to as the conventional SNCF here, through Neuber's rule [1-7], Glinka's method [3, 5, 7, 8] or linear rule [2, 4, 5, 9]. Comparison of the predicted values with finite element and experimental ones indicates that no rule can accurately predict the magnitude of the axial strain at the notch root. In particular, in notched rectangular bars the accuracy of the prediction decreases with increasing the thickness. The reason for this is that the conventional SNCF is defined under the uniaxial stress state [10], while the axial strain at the notch root occurs under the triaxial stress state. Strain-concentration factor should thus be defined under the triaxial stress state at the net section.

A new SNCF has been proposed by Majima under axial tension [10]. This new SNCF has been defined under the triaxial stress state at the net section. This has enabled the new SNCF to provide the reasonable values consistent with concave distributions of the axial strain on the net section [10, 11]. Moreover, this new SNCF has removed the contradiction that the conventional SNCF has the values less than unity for the concave distributions of the axial strain under elastic-plastic deformation. As mentioned earlier, the average axial strain or the nominal strain of the conventional SNCF has been defined under the uniaxial stress state; completely unrelated to the stress state at the net section [10, 11]. This causes the above contradiction of the conventional SNCF. This result indicates that the SNCF for any type of loading should be defined under the triaxial stress state at the net section.

Some studies have been made on the interference effect on the elastic stress-concentration factor (SSCF) of the flat bars with double U- or semicircular notches under tension. The obtained relations between the elastic SSCF and the notch pitch have been published for engineering design [12]. The important thing deduced from these studies is that the SSCF subjected to the interference effect is less than the SSCF of a single notch. Few studies have been carried out on the interference effect on the elastic SSCF of cylindrical bars with double U- or semicircular notches under tension [12]. Moreover, only two studies have been performed on the interference effect on strength such as yield point load and ultimate tensile strength and deformation properties of notched bars under tension [13, 14]. In these studies the interference effect has also been discussed on the elastic SSCF of cylindrical bars with double U-notches under tension.

In this paper the slant notch is employed to study the interference effect on the elastic-plastic SNCF accordingly. This is because the slant notch is closely related to the cracks growing in the slant direction.

2. Strain-Concentration Factor under Static Tension

The new strain-concentration factor (SNCF) proposed for tensile loading is given by [10]

$$K_{\varepsilon}^{\text{new}} = \frac{(\varepsilon_z)_{max}}{(\varepsilon_z)_{\text{av}}^{\text{new}}} \qquad (2\text{-}1)$$

where $(\varepsilon_z)_{\max}$ and $(\varepsilon_z)_{\text{av}}^{\text{new}}$ are the maximum axial strain at the notch root and the new average axial or new nominal strain, respectively. The maximum axial strain at the notch root is independent of definition, and hence the new SNCF depends on a new definition of the average axial strain. For circumferentially notched cylindrical bars $(\varepsilon_z)_{\text{av}}^{\text{new}}$ is defined as follows [10]:

$$\begin{aligned}(\varepsilon_z)_{\text{av}}^{\text{new}} &= \frac{1}{\pi r_n^2}\int_0^{r_n} \varepsilon_z(r)\, 2\pi r\, dr \\ &= 2\int_0^1 \varepsilon_z(s)\, s\, ds\end{aligned} \qquad (2\text{-}2)$$

where $s = r/r_n$. In the elastic level of deformation, $(\varepsilon_z)_{\text{av}}^{\text{new}}$ can be transformed into the following equation:

$$\begin{aligned}(\varepsilon_z)_{\text{av}}^{\text{new}} &= \frac{1}{\pi r_n^2}\int_0^{r_n} [\frac{\sigma_z}{E} - \frac{\nu}{E}(\sigma_\theta + \sigma_r)]\, 2\pi r\, dr \\ &= \frac{1}{E}\cdot\frac{1}{\pi r_n^2}\int_0^{r_n}\sigma_z\, 2\pi r\, dr - \frac{\nu}{E}\cdot\frac{1}{\pi r_n^2}\int_0^{r_n}(\sigma_\theta+\sigma_r)\, 2\pi r\, dr \\ &= \frac{1}{E}\cdot\frac{P}{\pi r_n^2} - \frac{\nu}{E}\cdot\frac{1}{\pi r_n^2}\int_0^{r_n}(\sigma_\theta+\sigma_r)\, 2\pi r\, dr \\ &= \frac{(\sigma_z)_{\text{av}}}{E} - \frac{\nu}{E}\cdot\frac{1}{\pi r_n^2}\int_0^{r_n}(\sigma_\theta+\sigma_r)\, 2\pi r\, dr\end{aligned} \qquad (2\text{-}3)$$

where E and ν are the Young's modulus and Poisson's ratio, respectively. Equation (2-3) can be rewritten as follows:

$$(\varepsilon_z)_{\text{av}}^{\text{new}} = \frac{(\sigma_z)_{\text{av}}}{E} - \frac{2\nu}{E}\int_0^1 \{\sigma_\theta(s)+\sigma_r(s)\}\, s\, ds \qquad (2\text{-}4)$$

This equation indicates that $(\varepsilon_z)_{\text{av}}^{\text{new}}$ is defined under the triaxial stress state at the net section. It should be noted that $(\varepsilon_z)_{\text{av}}^{\text{new}}$, given by Eq. (2-2), is defined under the triaxial stress state also in plastically deformed area at the net section. This is due to the following reason: the plastic component of the axial strain is directly related to the triaxial stress state, as indicated by the theory of plasticity. The definition under the triaxial stress state gives reasonable results consistent with the concave distribution of the axial strain at any deformation level [10, 11].

The conventional SNCF under static tension has been defined as the ratio of the maximum axial strain $(\varepsilon_z)_{\max}$ at the notch root to the conventional average axial strain $(\varepsilon_z)_{\text{av}}^{\text{con}}$, i.e.

$$K_{\varepsilon}^{\text{con}} = \frac{(\varepsilon_z)_{\max}}{(\varepsilon_z)_{\text{av}}^{\text{con}}} \qquad (2\text{-}5)$$

This conventional SNCF has been defined under uniaxial stress state at the net section. This is because the conventional average axial strain $(\varepsilon_z)_{\text{av}}^{\text{con}}$ has been defined under uniaxial stress state [10]. In elastic deformation, the axial stress σ_z at the notch root $(\sigma_z)_{\max}$ is much greater than $(\sigma_z)_{\text{av}}$, and the equivalent stress at the notch root $(\sigma_{\text{eq}})_{\max}$ is

a little lower than $(\sigma_z)_{max}$ under the biaxial tensile stress state. This indicates that the small plastic deformation occurs around the notch root even in the range $(\sigma_z)_{av} \leq \sigma_Y$, when $(\sigma_z)_{av}$ approaches σ_Y. Even in this range $(\varepsilon_z)_{av}^{con}$ is given by

$$(\varepsilon_z)_{av}^{con} = \frac{(\sigma_z)_{av}}{E} \qquad (2\text{-}6)$$

This equation indicates that the conventional definition has neglected the effect of tangential and radial stresses σ_θ and σ_r, respectively. On further development of plastic deformation, i.e. in the range $(\sigma_z)_{av} > \sigma_Y$, $(\varepsilon_z)_{av}^{con}$ is determined using the uniaxial true stress–total strain curve $\sigma = f(\varepsilon)$. The reason for using this curve is that $(\varepsilon_z)_{av}^{con}$ is defined under the uniaxial stress state and $(\sigma_z)_{av}$ is based on the instantaneous area of the net section. The conventional average axial strain is therefore given by

$$(\varepsilon_z)_{av}^{con} = f^{-1}\{(\sigma_z)_{av}\} \qquad (2\text{-}7)$$

As the plastic deformation develops from the notch root; i.e. $\sigma_{eq} > \sigma_Y$, the newly defined average axial strain has been calculated using the incremental or flow theory, which relates the stresses to the plastic strain increments. In the plastic deformation the strains in general are not uniquely determined by the stresses but depend on the entire history of loading.

3. Geometries and Materials

3.1. Geometries

The employed cylindrical bar with double-slant circumferential U-notches is shown in Fig. 1. The net-section diameter d_o of 10.0 mm and the gross diameter D_o of 16.7 mm were selected to give the net-to-gross diameter ratio d_o/D_o of 0.6. The specimen length is expressed as $(2L_o+2lo)$, where $2L_o$ and $2l_o$ are the unnotched length from the notch to the loaded end and the notch pitch, as shown in Fig. 1. The unnotched length L_o is 25 mm, held constant, while the half notch pitch l_o is varied from 0.0 to 12.5 mm to examine the interference effect of the double-slant circumferential U-notches. The notch pitch $2l_o$= 0.0 mm means a cylindrical bar with a circumferential V-notch, perpendicular to the axial direction. Two notch radii ρ_o of 0.5 and 1.0 mm are employed to vary the notch sharpness $d_o/2\rho_o$. The calculations were made on the double-slant circumferential U-notches of the slant angle of $\gamma = 45^o$.

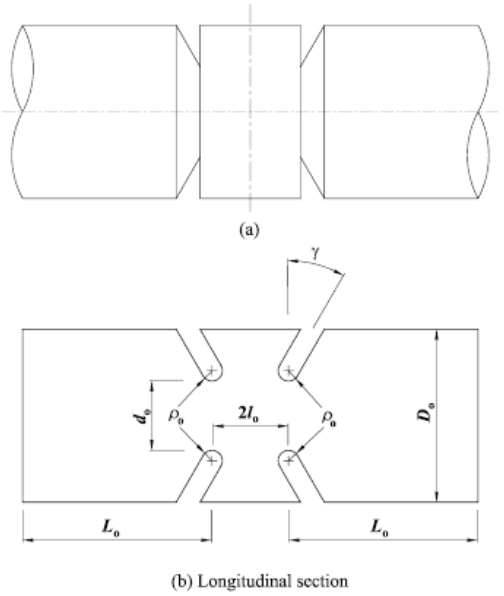

Figure 1: Cylindrical bar with double-slant circumferential U-notches.

3.2. Materials

The material employed is an Austenitic stainless steel. Young's modulus E, Poisson's ratio ν and the tensile yield stress σ_Y are listed in Table 1. The true stress-plastic strain curves were obtained from tension tests. In order to express the stress-strain curve accurately the obtained relation was divided into a few ranges of plastic strain and in each range the following fifth-degree polynomial was fitted:

$$\sigma = C_o + C_1\varepsilon_p + C_2\varepsilon_p^2 + C_3\varepsilon_p^3 + C_4\varepsilon_p^4 + C_5\varepsilon_p^5$$

The values of these coefficients in the plastic strain ranges used are also listed in Table 1. Figure 2 shows the true stress-plastic strain curve given by this polynomial.

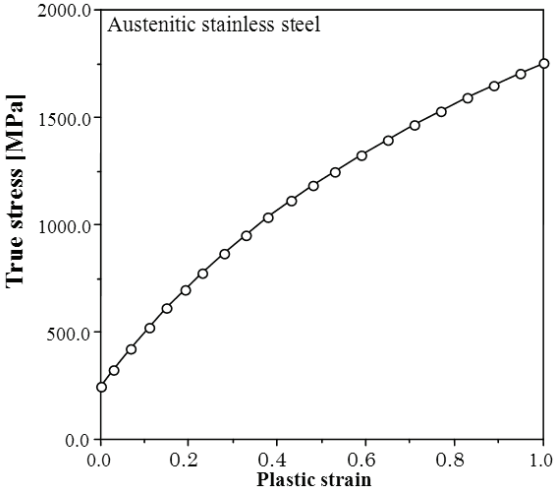

Figure 2: True Stress-strain curve for the plastic range of the material used.

Table 1: Mechanical properties and polynomial coefficients

Material ν, E [GPa], σ_Y [MPa]	Plastic strain range	C_o	C_1	C_2	C_3	C_4	C_5
Austenitic stainless steel	$\varepsilon_p \le 0.2$	2.459×10^2	4.389×10^3	-3.265×10^4	2.402×10^5	-8.899×10^5	1.258×10^6
0.30, 206, 245.9	$0.2< \varepsilon_p \le 0.5$	3.789×10^2	1.535×10^3	1.173×10^3	-1.874×10^3	0.0	0.0

4. Finite Element Mesh For Double-Slant Circumferential U-Notches

Figure 3 shows a finite element mesh of one quarter of a notched specimen with the double-slant circumferential U-notches. An eight-node axisymmetric ring element was chosen to model the notched specimens. The number of elements and nodes are given in Table 2 for ρ_o = 0.5 mm and in Table 3 for ρ_o =1.0 mm.

Table 2: Finite element mesh parameters for the double-slant circumferential U-notches of γ = 45° and ρ_o = 0.5 mm

l_o [mm]	L_o+l_o [mm]	No. of elements r × z	No. of elements Total	No. of nodes
0	25.0	18 × 28	504	1605
0.5	25.5	18 × 33	594	1885
1.5	26.5	18 × 39	702	2221
2.0	27.0	18 × 39	720	2277
2.5	27.5	18 × 41	738	2333
3.0	28.0	18 × 41	738	2333
3.5	28.5	18 × 41	738	2333
4.0	29.0	18 × 42	756	2389
5.0	30.0	18 × 42	756	2389
7.5	32.5	18 × 42	756	2389
10.0	35.0	18 × 44	792	2501
12.5	37.5	18 × 45	810	2551

Table 3: Finite element mesh parameters for the double-slant circumferential U-notches of γ = 45° and ρ_o =1.0 mm

l_o [mm]	L_o+l_o [mm]	No. of elements r × z	No. of elements Total	No. of nodes
0.0	25.0	18 × 28	504	1605
0.5	25.5	18 × 28	504	1605
1.0	26.0	18 × 35	630	1997
2.0	27.0	18 × 39	702	2221
2.5	27.5	18 × 41	738	2333
3.0	28.0	18 × 41	738	2333
4.0	29.0	18 × 43	774	2450
5.0	30.0	18 × 43	774	2450
7.5	32.5	18 × 43	774	2450
10.0	35.0	18 × 45	810	2557
12.5	37.5	18 × 47	846	2669

The FEM calculations were performed under the axisymmetric deformation; this deformation was given under the condition that the axial displacement at the gross section in the center of the notch pitch and the radial displacement at the central axis are zero. The increments of the axial displacement were applied at the right end of the unnotched part of $2L_o$. The magnitude of the increment was small enough to provide an elastic solution for the first few increments in each notched specimen. All of the calculations were performed using MARC K6.2 on an APOLLO workstation.

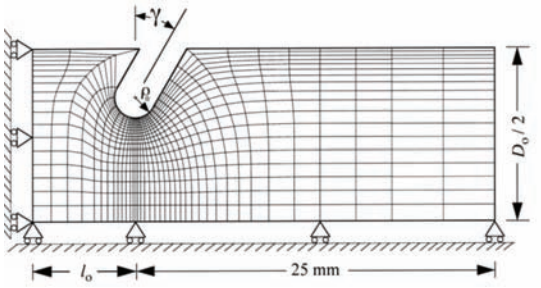

Figure 3: Finite element mesh of cylindrical bar with double-slant circumferential U- notches

5. Results and Discussion

5.1. Interference effect on the elastic new SNCF K_ε^{new}

Figure 4 shows the relation between the elastic new SNCF K_ε^{new} and half notch pitch l_o. The half notch pitch l_o = 0.0 mm means the single circumferential V-notch with the notch angle of 2γ. The elastic K_ε^{new} decreases very rapidly from the value at the half notch pitch l_o = 0.0 mm and reaches its minimum at $l_o \approx$ 0.5 mm. On further increase in l_o the elastic K_ε^{new} gradually increases and finally reaches the value of the single circumferential V-notch (l_o = 0.0 mm) at $l_o \approx$ 7.5 mm. Beyond this value of l_o the elastic K_ε^{new} is nearly constant up to l_o = 12.5 mm, the maximum half notch pitch in the FEM calculations. The elastic K_ε^{new} in the range 7.5 mm $\le l_o \le$ 12.5 mm are nearly equal to the elastic K_ε^{new} of the circumferential V-notch (l_o = 0.0 mm). This indicates that the interference effect on the elastic K_ε^{new} is extremely strong in a small range of l_o and nearly vanishes beyond $l_o \approx$ 7.5 mm.

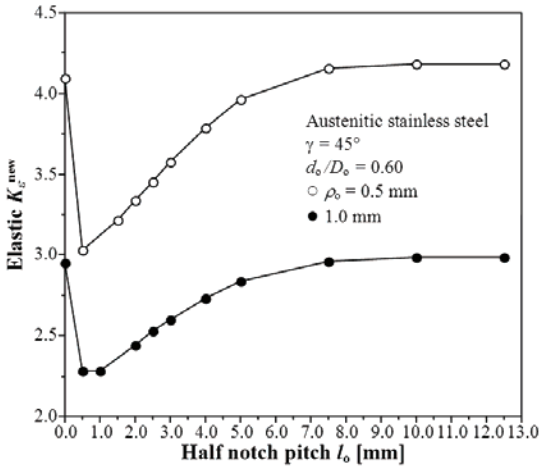

Figure 4: Effect of the half notch pitch l_o on the elastic K_ε^{new}

The variations in the maximum axial strain $(\varepsilon_z)_{max}$ and the new average axial strain $(\varepsilon_z)_{av}^{new}$ with tensile load P are shown in Fig. 5. It should be noted that plastic deformation already started at the notch root in the range $P \geq 7.5$ kN, Fig. 5. The maximum axial strain shows a strong dependence on the half notch pitch l_o in the elastic deformation, while the new average axial strain is nearly independent of l_o. The maximum axial strain at $l_o = 0.5$ mm is less than that for any other notch pitch, and hence the minimum elastic K_ε^{new} occurs at $l_o = 0.5$ mm. On the other hand, the maximum axial strain at $l_o = 12.5$ mm is greater than that at any other notch pitch and nearly equal to that at $l_o = 0.0$ mm. The maximum elastic K_ε^{new} thus occurs at $l_o = 0.0$ and 12.5 mm.

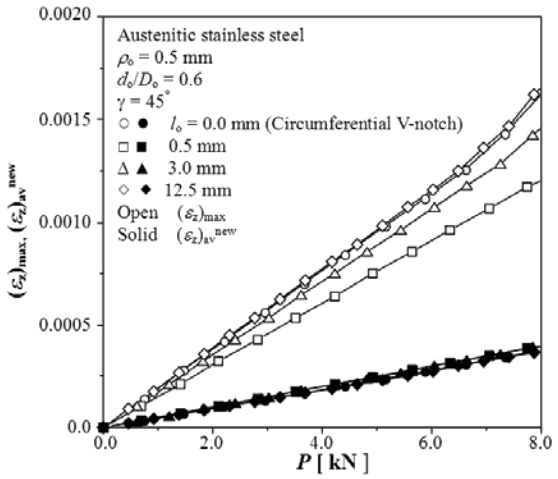

Figure 5: Effect of half notch pitch l_o on the variations in $(\varepsilon_z)_{max}$ and $(\varepsilon_z)_{av}^{new}$ with P at elastic deformation

5.2. Interference effect on the variations in K_ε^{new} with P

The variations in the new SNCF K_ε^{new} with tensile load P for $\rho_o = 0.5$ and 1.0 mm are given in Figs. 6 and 7, respectively. The results are shown for the double-slant circumferential U-notches of the slant angle $\gamma = 45°$ and of the notch radii $\rho_o = 0.5$ and 1.0 mm. The new SNCF increases from its elastic value. There is a load range where the rate of increase in the new SNCF decreases for the notch radius of 0.5 mm; this load range is independent of notch pitch. On further increase in tensile load the new SNCF rapidly increases again up to the maximum value and decreases. Approximately the same results were obtained for $l_o = 7.5$ and 10 mm.

For the notch radius of 1.0 mm the new SNCF increases from its elastic value to the peak value except for $l_o = 0.5$ to 2.5 mm. In these half notch pitches the gradual increase in the new SNCF is maintained in the load range where the peak value occurs for $l_o = 0.0$ and 3.0 to 12.5 mm. On further increase in tensile load the new SNCF rapidly increases again up to the maximum value, much greater than the peak value, and decreases after that. Approximately the same results were obtained for $l_o = 7.5$ and 10 mm.

The value of the tensile load P producing the maximum K_ε^{new} tends to increase with increasing l_o in the half notch pitch range from 0.5 to 12.5 mm. Furthermore, the value of P at the maximum K_ε^{new} of l_o=12.5 mm is approximately the same as that of l_o= 0 mm, the single circumferential V-notch.

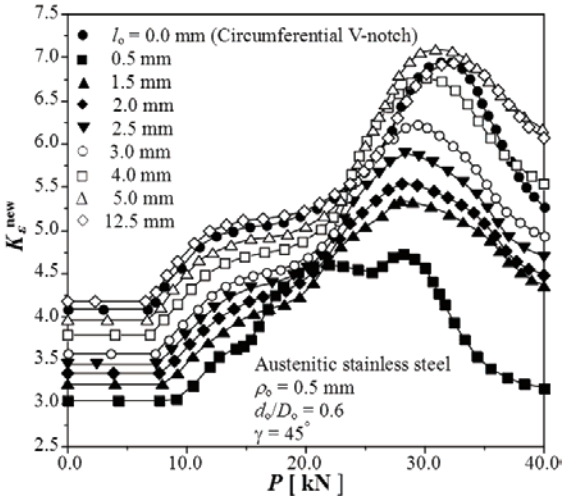

Figure 6: Effect of the half notch pitch l_o on the variations in K_ε^{new} with P for ρ_o=0.5 mm

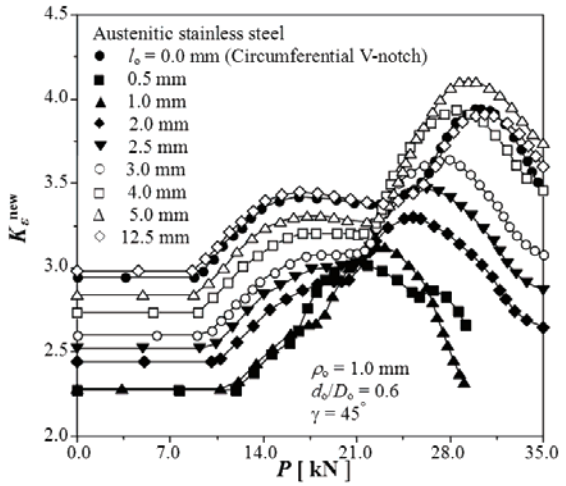

Figure 7: Effect of the half notch pitch l_o on the variations in K_ε^{new} with P for ρ_o=1.0 mm

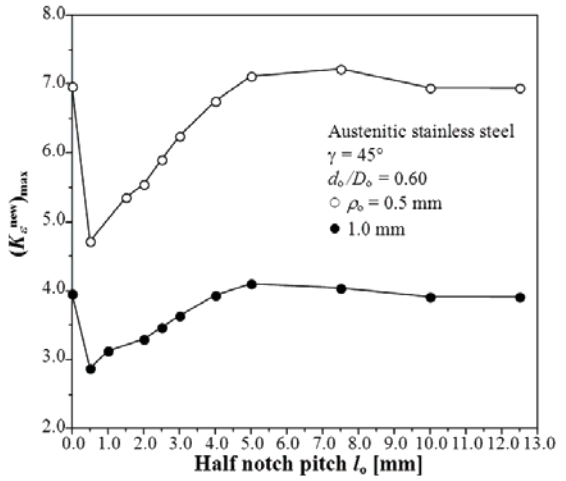

Figure 8 Effect of the half notch pitch l_o on $(K_\varepsilon^{new})_{max}$

  - Volume 1, Number 2 (ISSN 1995-6665)

This means that the maximum half notch pitch where the interference effect occurs on the maximum new K_ε^{new} is l_o= 12.5 mm. Figure 8 however shows that the half notch pitch where the interference effect occurs on the maximum new K_ε^{new} is much less than the half notch pitch of 12.5 mm; Fig. 8 shows the maximum new SNCF $(K_\varepsilon^{new})_{max}$ versus l_o relation for ρ_o = 0.5 and 1 mm. The relation between $(K_\varepsilon^{new})_{max}$ and l_o is remarkably similar in shape to that between the elastic K_ε^{new} and l_o. The maximum K_ε^{new} decreases very rapidly from its value at l_o= 0 mm to the minimum value at l_o= 0.5 mm. On further increase in l_o the maximum new SNCF increases and reaches the maximum value at l_o= 7.5 mm for ρ_o = 0.5 mm and at l_o = 5.0 mm for ρ_o = 1 mm. The values of the maximum K_ε^{new} of l_o = 10.0 and 12.5 mm are nearly equal to (ρ_o = 0.5 mm) or slightly less (ρ_o = 1.0 mm) than that of l_o = 0 mm, the single circumferential V-notch.

The new SNCF at l_o= 0.5 mm is the minimum value at any deformation level because the maximum axial strain of l_o = 0.5 mm is the smallest of all the notch pitches, as shown in Fig. 9. This is independent of notch radius. It should be noted that the maximum axial strain depends on l_o, while the new average axial strain is independent of l_o up to P = 25.0 kN, beyond which $(K_\varepsilon^{new})_{max}$ occurs. In the notched tension specimens, the plastic deformation is localized in a very narrow zone and spreads from notch root to the net section center. As a result, the maximum axial strain lies at the notch root [10, 13, and 14]. However, the current results indicate that this localization is prominent when the notch pitch becomes greater than 7.5 mm.

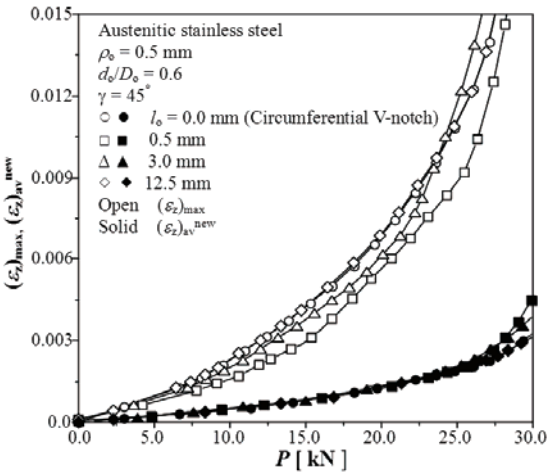

Figure 9: Effect of the half notch pitch l_o on the variation in $(\varepsilon_z)_{max}$ and $(\varepsilon_z)_{av}^{new}$ with P

This occurs because the notches with minimum pitches, i.e. $l_o \leq$ 7.5mm, produce the smaller percentage of the deformed region with large plastic strain than the notches with $l_o >$ 7.5mm do. Moreover, the plastic deformation spreads in inclined direction from the notch root to the pitch center line, as shown in Fig. 10. Therefore, the maximum axial strain for l_o= 0.5mm is the minimum and the K_ε^{new} for the minimum pitch is the smallest at any level of deformation.

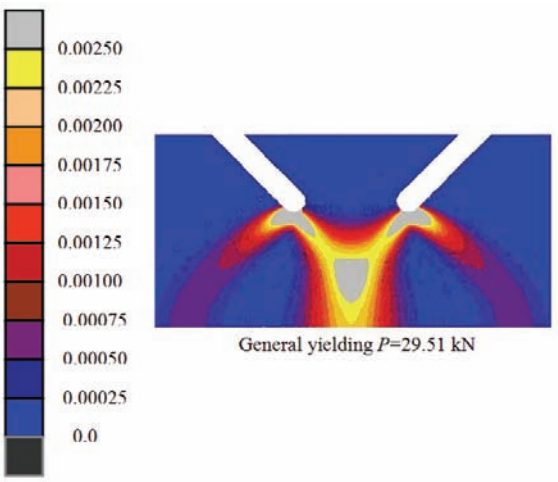

Figure 10: Distributions of the total equivalent plastic strain on the net section of double-slant circumferential U-notches with l_o=2.5 mm, ρ_o = 0.5 mm and γ =45°

6. Conclusions

The results given in Figs. 4 through 9 are of the double-slant circumferential U-notches of the slant angle γ = 45 and of two notch radii of 0.5 and 1.0 mm. The following conclusions can be drawn from the results:

1. The relation between the elastic new SNCF and half notch pitch l_o shows very rapid decrease from the value at l_o= 0 mm with increasing l_o. The elastic new SNCF becomes minimum at $l_o \approx$ 0.5 mm. On further increase in l_o the elastic new SNCF gradually increases and reaches the maximum value at $l_o \approx$ 7.5 mm. This maximum value is nearly equal to the elastic new SNCF at l_o = 0 mm. The elastic new SNCF is almost constant up to l_o = 12.5 mm for further notch pitch.
2. The relation between the maximum new SNCF in plastic deformation and l_o is remarkably similar in shape to that between the elastic new SNCF and l_o. The maximum notch pitch where the interference effect occurs on this maximum new SNCF tends to be less than the notch pitch where the interference effect occurs in the relation between the elastic new SNCF and l_o.
3. The new SNCF rapidly increases from its elastic value with increasing tensile load. It shows the peak value or the gradual increase after this rapid increase. On further increase in tensile load the new SNCF rapidly increases again to the maximum value and finally decreases. The maximum value is much greater than the peak value. Particularly, the ratio between the maximum value and the peak value of the new SNCF is varying form 1.1 to 1.75, i.e. nearly 1.1 for l_o=0.5 mm and 1.75 for l_o=12.5mm.

References

[1] W.N.Jr. Sharp, M. Ward, “Benchmark cyclic plastic notch strain measurements”. Trans. ASME, J. Engng Mater. Technol. Vol. 105, 1983, 235-241.

[2] A.R. Gowhari-anaraki, S.J. Hardy, “Low cycle fatigue life predictions for hollow tubes with axially loaded axisymmetric internal projections”. J. Strain Analysis, Vol. 26, 1991, 133-146.

[3] W.N.Jr. Sharp, “ASME 1993 Nadai Lecture-Elastoplastic stress and strain concentrations”. Trans. ASME, J. Engng Mater. Technol., Vol. 117, 1995, 1-7.

[4] S.J. Hardy, M.K. Pipelzadeh, “An assessment of the notch stress-strain conversion rules for short flat bars with projections subjected to axial and shear loading." Journal . Strain Analysis. Vol. 31, No. 2, 1996, 91-110.

[5] Z. Zeng, A. Fatemi, “Elasto-plastic stress and strain behaviour at notch roots under monotonic and cyclic loadings”. Journal Strain Analysis, Vol. 36, 2001, 287-288.

[6] G. Harkegard, T. Mann, “Neuber prediction of elastic-plastic strain concentration in notched tensile specimens under large-scale yielding”. J. Strain Analysis, Vol. 38, 2003, 79-94.

[7] P. Livieri, G.. Nicoletto, “Elastoplastic strain concentration factors in finite thickness plates”. J. Strain Analysis, Vol. 38, 2003, 31-36.

[8] G. Glinka, “Energy density approach to calculation of inelastic strain-stress near notches and cracks”. Engng Fracture Mechanics, Vol. 22, 1985, 485-508.

[9] H.O Fuchs, R.L.Stephens, ,. Metal fatigue in engineering. New York: John Wiley and Sons; 1980.

[10] T. Majima, “Strain-concentration factor of circumferentially notched cylindrical bars under static tension”. Journal Strain Analysis, Vol. 34, No. 5, 1999, 347-360.

[11] H. M. Tlilan, S. Yousuke, T. Majima, “Effect of notch depth on strain-concentration factor of notched cylindrical bars under static tension”, European Journal of Mechanics A/Solids. Vol. 24 , 2005, 406-416.

[12] W.D. Pilkey. Peterson’s stress concentration factors. New York: Wiley; 1997.

[13] T. Majima, “Interference effect of notches (1st report, evaluation of interference effect of notches on yield point load of double U-shaped notches by upper and lower bound theorems)”. *Trans. Japan Soc. Mech. Engrs*., Vol. 48, No. 430, 1982, 719-728.

[14] T. Majima, K. Watanabe, “Interference effect of notches (2nd report, an experimental investigation of interference effect on strength and deformation properties of notched bars with double symmetrical u-notches)”. *Trans. Japan Soc. Mech. Engrs*. Vol. 48, No. 433, 1982, 1186-1194.